

Application of weak ferromagnetic BiFeO₃ films as the photoelectrode material under visible-light irradiation

X. Y. Chen, T. Yu,^{a)} F. Gao, H. T. Zhang, L. F. Liu, Y. M. Wang, Z. S. Li, and Z. G. Zou
Eco-Materials and Renewable Energy Research Center, National Laboratory of Solid State Microstructures, Nanjing University, Nanjing 210093, People's Republic of China

J.-M. Liu

National Laboratory of Solid State Microstructures, Nanjing University, Nanjing 210093, People's Republic of China and International Center for Materials Physics, Chinese Academy of Sciences, Shenyang 110015, People's Republic of China

(Received 6 February 2007; accepted 20 June 2007; published online 13 July 2007)

BiFeO₃ films prepared by pulsed laser deposition on Pt/TiO₂/SiO₂/Si substrates were studied as photoelectrode for water splitting. Under visible-light irradiation, the photocurrent intensity of the polycrystalline BiFeO₃ film was found to double that of the amorphous one in a three-electrode cell. The incident photon to current conversion efficiency for the polycrystalline BiFeO₃ electrode was approximately 16% at 350 nm and 7% at 530 nm at 1.5 V (versus saturated calomel electrode). The ferromagnetism of the amorphous BiFeO₃ film was an order of magnitude weaker than that of the polycrystalline one, supporting the "size effect" explanation for magnetic origin. © 2007 American Institute of Physics. [DOI: 10.1063/1.2757132]

In recent years, as a kind of multiferroic material, BiFeO₃ (BFO) has been widely researched because of its promising magnetoelectric application at room temperature (RT).¹⁻³ Particularly, the small band gap of BFO (~2.2 eV) has also attracted increasing attention because it is possible for us to explore BFO as an efficient visible-light photocatalytic material.^{2,4,5} Recently, we have observed the photoinduced oxidization ability of BFO nanowires,² and significant photocatalytic pollutant decomposition properties of BFO nanoparticles,⁴ suggesting that BFO might be a promising material as photoelectrode for water photoelectrolysis. Since the discovery of water splitting on a TiO₂ photoelectrode in 1972, photoelectrolysis of water has become one of the most promising techniques for solar energy conversion and storage.⁶ Oxide semiconductors have many advantages for this application because they are generally stable and produced easily compared with nonoxide semiconductors.⁹ Among them, α -Fe₂O₃ and WO₃ have been widely studied because they have small energy band gaps (2.0 and 2.7 eV, respectively) to absorb visible light.⁸⁻¹⁰ However, the number of photoelectrode materials working under visible-light irradiation is still limited. In this letter, we report the significant photocurrent performance of the polycrystalline and the amorphous BFO films under visible-light irradiation. We also measured the magnetic property of the amorphous BFO film to help us understand the magnetic origin in BFO.

The BFO photoelectrode films were prepared by pulsed laser deposition (PLD), which was reported in our previous publications.^{11,12} In this study, the BFO films were prepared on commercial Pt/TiO₂/SiO₂/Si substrates in the fixed optimized oxygen atmosphere of 10 Pa, while the substrate temperature was kept at $T_s=300$ or 550 °C. To examine the structure of the PLD-grown BFO thin films, x-ray diffraction (XRD) and Raman spectra measurements were carried out. The optical transmission property of the BFO films was stud-

ied using UV-visible transmission spectra by depositing BFO on quartz glass substrates under the same condition. All photoelectrochemical measurements were performed in a three-electrode pyrex glass cell. The prepared films on Pt/TiO₂/SiO₂/Si substrates were used as the work electrode. A Pt wire and a saturated calomel electrode (SCE) were used as the counter and the reference electrode, respectively. A 0.2M Na₂SO₄ aqueous solution ($pH \approx 7.5$) was used as the electrolyte. The light source was a 400 W Xe lamp covered with a 420 nm cutoff filter to remove the light with wavelength less than 420 nm. The incident photon to current conversion efficiency (IPCE) was obtained under different irradiation by employing monochrome filters.

The BFO film deposited at $T_s=300$ °C was found to be in an amorphous phase and no peaks except those from the substrate were observed in the XRD pattern shown in Fig. 1. By increasing the T_s to 550 °C, the BFO film was found to be polycrystalline with perovskite structure. No impurity phase except for a trait of Bi₄Fe₂O₉ was observed. The Raman spectra of the BFO films deposited at different temperatures are shown in the inset of Fig. 1. Two intense peaks at 174 and 223 cm⁻¹ were observed in the polycrystalline film, similar to that of 168 and 212 cm⁻¹ observed in a 600-nm-thick (001)-oriented epitaxial BFO thin film.¹³ Those two peaks were also observed in the amorphous BFO film although the peak intensity was much weaker. Since it was reported that amorphous ferrites contain microcrystalline domains in the amorphous matrix,¹⁴ we infer that there existed small BFO crystalline domains in the amorphous BFO film. In addition, neither peaks assigned to α -Fe₂O₃ crystallographic phase nor those assigned to Bi₂O₃ were observed in both films,^{8,15} indicating that such impurity phases were neglectable in both our films, consistent with our XRD result.

The BFO films deposited on quartz glass substrates were transparent with a brown color. The UV-visible transmission spectra result is shown in the inset of Fig. 2(a). It is found that both the polycrystalline and the amorphous BFO films

^{a)} Author to whom correspondence should be addressed; electronic mail: yutao@nju.edu.cn

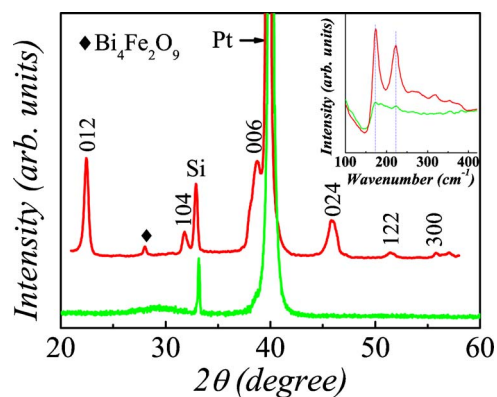


FIG. 1. (Color online) XRD pattern and Raman spectra (inset) of the BFO films prepared by PLD deposited at $T_s=550$ °C (top line) and 300 °C (bottom line).

had a strong absorbance in the visible-light region. The optical transmission spectra of the polycrystalline BFO film were similar with that of a 300-nm-thick BFO film prepared by a thermal pyrolysis method.¹⁶ The band gaps of the BFO films were estimated by plotting the curve of $(-\ln T)^{1/2}$ and $(h\nu)$ according to the following expression:¹⁰

$$(-\ln T)^n \propto A^n d^n (h\nu - E_g), \quad (1)$$

where T is the transmission value, A is the proportional constant, d is the thickness of the film, and $h\nu$ is the energy of the incident photon. n is $1/2$ for BFO, which is an indirect band gap semiconductor.¹⁷ The obtained energy band gaps were 2.1 and 2.0 eV for the polycrystalline and the amorphous film, both somewhat smaller than that of the BFO nanoparticles (2.18 eV).⁴

Figure 2(a) shows the photocurrent spectra recorded for the different BFO photoelectrodes under visible-light irradiation. The irradiation of visible light ($\lambda > 420$ nm, 60 mW cm^{-2}) was chopped at a frequency of 0.33 Hz. The photocurrent is calculated by subtracting the current in the dark from the current under irradiation. For the polycrystalline BFO electrode, the dark current intensity only increased to 9×10^{-6} A cm^{-2} when the applied potential increased to 1.5 V (versus SCE), while the current intensity increased to 1.59×10^{-4} A cm^{-2} under irradiation. The considerable anode photocurrent indicated that BFO could be referred to a n -type semiconductor,¹⁸ like most oxide semiconductors. Gentle rise of the photocurrent-potential curve was observed just like that of the BiVO_4 photoelectrode.⁷ It was suggested that the low conductivity was reasonable for such photocurrent character and it would be improved by a decrease in defects at the grain boundary.⁷ On our amorphous BFO electrode, significant photocurrent intensity was also observed, although it was weaker than that of the polycrystalline BFO electrode. The dark current of the amorphous BFO electrode was much higher than that of the polycrystalline electrode, which was possibly caused by the direct contact of Pt substrate with the penetrated electrolyte.

The IPCE curves of the polycrystalline BFO electrode at different potentials are given in Fig. 2(b) and they are obtained by the equation described in other place.¹⁹ The IPCE curves all had a maximum value at 350 nm, corresponding to the maximum of the optical absorption. The IPCE values increased with increasing the applied potential, and at 1.5 V (versus SCE) they were approximately 16% at 350 nm and

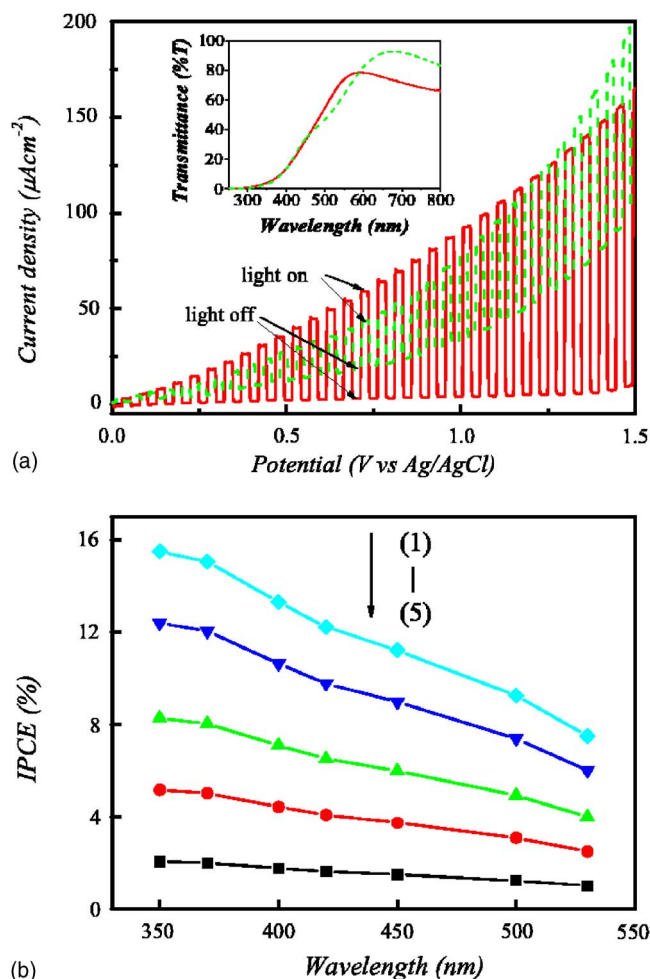


FIG. 2. (Color online) (a) Current-potential dependence of the BFO film electrode under visible-light irradiation. ($\lambda > 420$ nm, light intensity: 60 mW cm^{-2}). The inset presents optical transmission spectra of BFO films grown on quartz glass. (Solid line for the polycrystalline film and dashed line for the amorphous film.) (b) IPCE of the polycrystalline BFO film electrode measured at different potentials. (1) 1.5 V, (2) 1.2 V, (3) 0.8 V, (4) 0.5 V, and (5) 0.2 V.

7% at 530 nm. Duret and Grätzel reported that the $\alpha\text{-Fe}_2\text{O}_3$ film had IPCE values approximately 23% at 350 nm and 4% at 530 nm at 1.6 V (versus reversible hydrogen electrode) in 1M NaOH solution.⁸ Porous WO_3 electrode was reported with IPCE of approximately 33% at 350 nm and 0% at 530 nm in 0.1M H_2SO_4 solution at 1.5 V (versus Ag/AgCl).¹⁰ BiVO_4 polycrystalline electrode had IPCE values approximately 58% at 350 nm and 0% at 530 nm at 1.3 V (versus reversible hydrogen electrode) in 0.5M Na_2SO_4 solution.⁷ Our polycrystalline BFO photoelectrode showed comparable efficiency with these traditional excellent photoelectrode materials. In addition, the advantage of our BFO films utilizing long wavelength photons is obvious, especially comparing with WO_3 and BiVO_4 . It is reasonable because WO_3 and BiVO_4 have too large energy band gaps (2.7 and 2.4 eV, respectively) to absorb the light of 530 nm (2.3 eV).

Some ferrites have been studied as photoelectrode materials, such as YFeO_3 , CdFe_2O_4 , and $\text{PbFe}_{12}\text{O}_{19}$.²⁰ They were reported to be chemically stable but with poor light response. Herein, we examined the chemical stability of BFO photoelectrode by inductively coupled plasma mass spectrometry. The electrolyte solutions after the IPCE measurement was

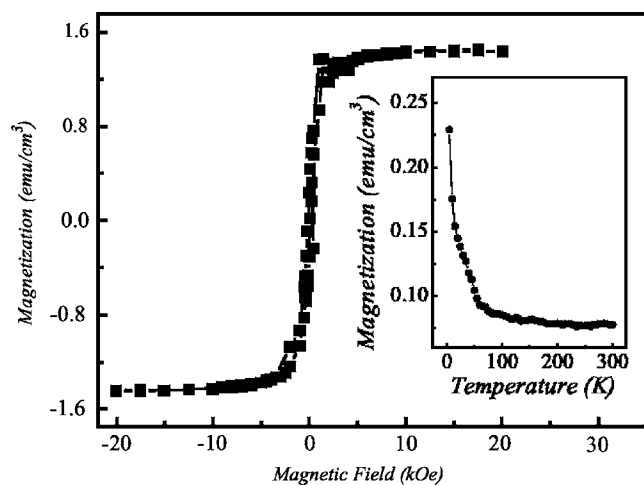


FIG. 3. M - H hysteresis loop of the amorphous BFO film measured at room temperature. The inset shows the temperature dependent magnetization of the amorphous BFO film.

analyzed, and the elements Bi or Fe were not found. As for the reason of such a high efficiency of our polycrystalline BFO electrode, we consider Bi orbitals in this ferrite probably have played important roles. It is suggested that the transfer of holes in the valence band becomes easy by the formation of hybrid Bi $6s$ -O $2p$ orbital.⁷ In fact, BiVO₄ was reported to be an excellent photoelectrode material with high efficiency, while in YVO₄ and InVO₄ electrodes, high efficiencies were not obtained.

Considering the importance of magnetic origin of BFO, we also investigated the magnetic behavior of the amorphous BFO film. The magnetization M as a function of both the magnetic field H and the temperature T was obtained using the superconducting quantum interference device magnetometer. As shown in Fig. 3, weak FM order was observed for our amorphous BFO film at RT, similar to the magnetic behavior of crystalline BFO film.³ However, the magnetization of the amorphous film was about one order of magnitude lower than that of the crystalline one. As discussed above, our amorphous film contained crystalline nanodomains. Combining the suggestion that the nanodimension might be responsible for the FM order in BFO,^{2,4,21} one may argue that it is the BFO crystalline domains that contribute to the weak FM in the amorphous BFO film. Since the crystalline domains in the amorphous film only occupy a small fraction of the whole film,¹⁴ it is reasonable that the magnetization is much smaller than that in the crystalline film. We also performed the temperature demagnetization-magnetization measurement (M - T) under $H=2000$ Oe. As shown in Fig. 3 (inset), M remains nearly constant as T goes down from RT to around 70 K, below which we see an unusual rapid rising, which was attributed to the spin glass behavior.¹² Such a M - T curve is similar to that of the BFO based films and BFO ceramics,¹² which further supports our suggestion that the

nanocrystalline BFO domains be responsible for the weak FM.

In summary, we investigated the photocurrent performance of the PLD-grown BFO electrode films. The polycrystalline BFO electrode was proved to be suitable for photoelectrode application, which showed high IPCE values under visible-light irradiation especially in the region of long wavelength. Moreover, weak ferromagnetism was observed in the amorphous BFO film, providing a further evidence of our suggestion that the nanodimension (size effect) be responsible for the FM order in BFO nanostructures.

The authors would like to acknowledge the financial support from the National Natural Science Foundation of China (Nos. 20603017 and 20528302), the National Key Projects for Basic Research of China (2002CB613303 and 2006CB921802), the Jiangsu Provincial Natural Science Foundation of China (Nos. BK2006718 and BK2006127), and the Jiangsu Provincial High Technology Research Project (No. BG2006030). Two of the authors (Z.G.Z. and T.Y.) would like to thank the Talent Project of the Jiangsu Province.

- ¹J. Wang, J. B. Neaton, H. Zheng, V. Nagarajan, S. B. Ogale, B. Liu, D. Viehland, V. Vaithyanathan, D. G. Schlom, U. V. Waghmare, N. A. Spaldin, K. M. Rabe, M. Wuttig, and R. Ramesh, *Science* **299**, 1719 (2003).
- ²F. Gao, Y. Yuan, K. F. Wang, X. Y. Chen, F. Chen, J.-M. Liu, and Z. F. Ren, *Appl. Phys. Lett.* **89**, 102506 (2006).
- ³W. Eerenstein, F. D. Morrison, J. Dho, M. G. Blamire, J. F. Scott, and N. D. Mathur, *Science* **307**, 1203a (2005).
- ⁴F. Gao, X. Y. Chen, K. B. Yin, S. Dong, Z. F. Ren, F. Yuan, T. Yu, Z. G. Zou, and J.-M. Liu, *Adv. Mater. (Weinheim, Ger.)* (to be published).
- ⁵J. Lou and P. A. Maggard, *Adv. Mater. (Weinheim, Ger.)* **18**, 514 (2006).
- ⁶A. Fujishima and K. Honda, *Nature (London)* **238**, 37 (1972).
- ⁷K. Sayama, A. Nomura, Z. Zou, R. Abe, Y. Abe, and H. Arakawa, *Chem. Commun. (Cambridge)* **2003**, 2908.
- ⁸A. Duret and M. Grätzel, *J. Phys. Chem. B* **109**, 17184 (2005).
- ⁹S. Berger, H. Tsuchiya, A. Ghicov, and P. Schmuki, *Appl. Phys. Lett.* **88**, 203119 (2006).
- ¹⁰W. J. Luo, T. Yu, Y. M. Wang, Z. S. Li, J. H. Ye, and Z. G. Zou, *J. Phys. D* **40**, 1091 (2007).
- ¹¹F. Gao, C. Cai, Y. Wang, S. Dong, X. Y. Qiu, G. L. Yuan, Z. G. Liu, and J.-M. Liu, *J. Appl. Phys.* **99**, 094105 (2006).
- ¹²F. Gao, X. Y. Qiu, Y. Yuan, B. Xu, Y. Y. Weng, F. Yuan, L. Y. Lv, and J.-M. Liu, *Thin Solid Films* **515**, 5366 (2007).
- ¹³Y. B. Park, J. L. Ruglovsky, and H. A. Atwater, *Appl. Phys. Lett.* **85**, 455 (2004).
- ¹⁴S. Nakamura, N. Ichinose, and Y. Hirotsu, *Jpn. J. Appl. Phys., Part 2* **30**, L844 (1991).
- ¹⁵C. Chouinard and S. Desgreniers, *Solid State Commun.* **113**, 125 (2000).
- ¹⁶T. Kanai, S. I. Ohkoshi, and K. Hashimoto, *J. Phys. Chem. Solids* **64**, 391 (2003).
- ¹⁷J. B. Neaton, C. Ederer, U. V. Waghmare, N. A. Spaldin, and K. M. Rabe, *Phys. Rev. B* **71**, 014113 (2005).
- ¹⁸A. J. Bard and L. R. Faulkner, *Electrochemical Methods: Fundamentals and Applications* (Wiley, New York, 2002), Chap. 18, p. 754.
- ¹⁹H. Wang, T. Lindgren, J. He, A. Hagfeldt, and S. E. Lindquist, *J. Phys. Chem. B* **104**, 5686 (2000).
- ²⁰H. P. Marusk and A. K. Ghosh, *Sol. Energy* **20**, 443 (1978).
- ²¹T. J. Park, G. C. Papaefthymiou, A. J. Viescas, A. R. Moodenbaugh, and S. S. Wong, *Nano Lett.* **7**, 766 (2007).